

## An experimental study of solar air heater using arc shaped wire rib roughness based on energy and exergy analysis

HARISH KUMAR GHRTLAHRE\*

Department of Energy and Environmental Engineering,  
Chhattisgarh Swami Vivekanand Technical University,  
Bhilai, Chhattisgarh, 491107, India

**Abstract** In the present study, energy and exergy analysis has been evaluated for roughened solar air heater (SAH) using arc shaped wire ribs. To achieve this aim, two different types of flow arrangement have been considered. These arrangements are: apex upstream flow and apex downstream flow. In addition to this, a smooth duct SAH has been used for comparative study. The experiments were performed using the mass flow rate of 0.007–0.022 kg/s on outdoor condition at Jamshedpur city of India. The absorber plate roughness geometry has been designed with relative roughness height 0.0395, rib size 2.5 mm, relative roughness pitch 10 and arc angle  $60^\circ$ . The energetic and exergetic performances have been examined on the basis of the first and second law of thermodynamics. According to the results, there is observed to be the maximum thermal efficiency and exergy efficiency as 73.2% and 2.64%, respectively, for apex upstream flow SAH at 0.022 kg/s, while, at same mass flow rate the maximum thermal efficiency and exergy efficiency is obtained as 69.4% and 1.89%, respectively, for apex downstream flow SAH. In addition to this, results reported that the maximum outlet temperature and temperature difference observed at lower mass flow rate. Also examined the outlet air temperature of SAH with various mass flow rates is very important for both analysis.

**Keywords:** Artificial roughness; Arc shaped geometry; Energy analysis; Exergy analysis; Solar air heater

---

\*Corresponding Author. Email: [harish.ghritlahre@gmail.com](mailto:harish.ghritlahre@gmail.com)

## Nomenclature

$A_p$	–	absorber plat area, m <sup>2</sup>
$C_p$	–	specific heat, J/kgK
$e$	–	roughness size, mm
$e/D$	–	relative roughness height
$\dot{E}$	–	energy rate, W
$\dot{E}x$	–	exergy rate, W
$\dot{E}x_d$	–	irreversibility rate, W
$h$	–	enthalpy, J/kg
$I$	–	solar irradiance, W/m <sup>2</sup>
$\dot{m}$	–	mass flow rate, kg/s
$P$	–	pressure, Pa
$p/e$	–	relative roughness pitch
$\dot{Q}_c$	–	incident solar radiation, W
$\dot{Q}_u$	–	useful heat gain, W
$R$	–	universal gas constant, J/kgK
$s$	–	entropy, J/K
$T$	–	temperature, K

## Greek symbols

$\alpha$	–	absorptivity of absorber plate
$\eta_I$	–	energy efficiency
$\eta_{II}$	–	exergy efficiency
$\eta_{th}$	–	thermal efficiency
$\eta_{eff}$	–	effective efficiency
$\psi$	–	specific exergy, J/kg
$\tau$	–	transmissivity of glass cover

## Subscripts

$a$	–	air
$d$	–	destruction
$e$	–	environment
$ext$	–	external
$f$	–	fluid (air)
$fi$	–	inlet air
$fo$	–	outlet air
$fm$	–	mean air
$o$	–	outlet
$s$	–	sun

## Abbreviations

ANN	–	artificial neural network
SAC	–	solar air collector
SAH	–	solar air heater

## 1 Introduction

Solar energy is among the most promising sources of renewable energy as it is very helpful in the field of domestic and industrial applications. In solar thermal systems, solar air heater (SAH) is an important device for heating of air. It is specially used in space heating, timber seasoning, drying of agriculture farm product and drying purpose in paper mills and food industries etc. [1–4]. The collector or absorber plate plays a vital role in SAH which absorbs solar radiations in the form of heat and transmits to the flowing air. The main advantages of SAHs are low operating and maintenance cost, and its design is simple. On the other side, the performance of conventional SAH is very weak as the mutual heat transfer in the collector surface and flowing air is low. To improve this performance of SAH several researchers have used various types of techniques such as artificial roughness on collector surface, extended surfaces, honeycomb collectors and using packing on air flow side etc. to enhance the rate of heat transfer through convection by creating surface on absorber plate. Various types of roughness geometry were used by investigators such as arc shaped, transverse rib, W-shaped, C-shaped, V-shaped, S-shaped, inclined wire rib roughness, etc. [5, 6].

Using the 1st law of thermodynamics, the thermal and thermohydraulic performances of energy systems are examined. But, the 2nd law of thermodynamics is associated with irreversibility of an energy system. The concept of exergy analysis is very useful for evaluation of performance, design, and optimization of system [7–9].

Many researchers have used the concept of 1st and 2nd laws of thermodynamics. Kurtbas and Durmus designed five different kinds of solar air collectors (SACs) and examined the exergy and thermal efficiencies [10]. They reported that the pressure loss, difference between outlet and inlet temperatures of the fluid, roughness geometry and collector efficiency etc. are more important to examine the performances of SAH. Kurtbas and Turgut studied the thermal and exergy efficiency of SAH with fixed and free fins [11]. They reported that the fixed fin SAC performs better than free fin collector, also found that the heat transfer and exergy loss, both increases as the pressure loss increases. Karsli designed a novel type of SAC which is used for drying and evaluated the energetic and exergetic efficiencies [12]. For this aim, they developed experimental setup with four types of collectors such as finned collectors (Type-A: with 75° flow angle and Type –B: with 70° flow angle), Type-C: tube collector and Type –D: smooth collector with no obstacles, and found that the energy efficiency ( $\eta_I$ ) changed

from 26% to 80% for type-A, type-B: from 26% to 42%, type-C: from 60% to 70%, and type-D: from 26% to 64%. They obtained the exergy efficiency ( $\eta_{II}$ ) for all collectors as 0.27 and 0.64. Esen conducted an experiment with double flow SAC using with and without obstacles type absorber surfaces [13]. Author have used three various mass flow rate ( $\dot{m}$ ) as 0.015, 0.02, and 0.025 kg/s in the experiments. By applying the concept of energy and exergy, it was found that the obstacles type SAHs performs better as compared to SAH type case without obstacles at same operating conditions. Gupta and Kaushik studied the exergetic performance of flat-plate SAH to achieve optimal performance [14]. They analytically evaluated the rate of exergy input ( $\dot{E}x_{in}$ ) and output ( $\dot{E}x_{out}$ ) for different mass flow rate unit collector area, duct depths and aspect ratio. They found that maximum  $\dot{E}x_{out}$  is observed at minimum value of  $\dot{m}$  when the temperature of inlet air ( $T_{fi}$ ) is low. Gupta and Kaushik analytically studied the energy, exergy and effective efficiencies of various types of roughness [15]. They selected six different types of roughness such as wedge shaped rib (I), circular ribs (II), V-shaped ribs (III), chamfered rib-groove (IV), expanded metal mesh (V), and rib-grooved (VI). By the use of correlations they coded the program in Matlab software and calculated the  $\eta_I$ ,  $\eta_{II}$ , and the effective efficiency ( $\eta_{eff}$ ). They found that the efficiencies are improved by using roughness as compared to smooth surface (VII). Akpınar and Kocyigit developed a new design of SAH with and without obstacles and experimentally investigated the performances [16]. They conducted experiments using  $\dot{m}$  at 0.0052 and 0.0074 kg/s. After analyzing the 1st and 2nd laws of thermodynamics, it was reported that the thermal effective efficiency ( $\eta_{th}$ ) varies from 20% to 82% while the  $\eta_{II}$  varied from 8.32% to 44% at same operating condition. They also found that the solar intensity and geometry of absorber plate affects the efficiency of SAHs. Alta *et al.* [17] fabricated new design of SAHs and investigated the energy and exergetic efficiency. They constructed absorber plate using fins and without fins. They evaluated the thermal and exergy efficiency for collector without fin, with fins using single glass cover and double glass cover at three different mass flow rate at tilt angles with  $0^\circ$ ,  $15^\circ$ , and  $30^\circ$ . They found that the finned SAH with double glass cover was more effective due to the higher temperature difference as compared to without finned SAH.

Bouadila *et al.* [18] designed a novel type of packed bed SAH using spherical capsules for analysis of energetic and exergetic performance. To achieve this object they conducted experiments and applied 1st and 2nd laws of thermodynamics for calculating  $\eta_I$  and  $\eta_{II}$ . They found the net

daily increase of  $\eta_I$  from 32% to 45%, while the daily  $\eta_{II}$  from 13% to 25%. Benli applied the concept of 1st and 2nd laws of thermodynamics for evaluating the thermal and exergetic efficiency of new designed SAH with four different absorber surface [19]. Bayrak *et al.* [20] designed new type of SAH using porous baffles inserted. They used energy and exergy analysis method for SAH performance. They conducted experiments with two different  $\dot{m}$  such as 0.016 and 0.025 kg/s, and used five different cases such as Case I: smooth absorber, Case II: Non-staggered absorber with 6 mm baffle thickness, Case III: Staggered absorber with 6 mm baffle thickness, Case IV: Non-staggered absorber with 10 mm baffle thickness and Case V: Staggered absorber with 10 mm baffle thickness. From the experimental result, it was found that the maximum  $\eta_{th}$  and  $\eta_{II}$ , and temperature difference are obtained for 6 mm thickness of porous materials at  $\dot{m} = 0.025$  kg/s in case III, whereas the minimum values are found for the flat plate SAC at  $\dot{m} = 0.016$  kg/s in case I.

Velmurugan and Kalaivanan developed the energy balance equation for single, double, and triple pass SAHs to analyze the energetic and exergetic performances [21]. They programmed a simulation code in Matlab software for calculating the  $\eta_{th}$  and  $\eta_{II}$ . They studied the effect of  $\dot{m}$  on energetic efficiency, exergetic efficiency, improvement efficiency, irreversibility and rise in temperature difference. It was found that triple pass SAH performed better than the single and double pass SAH. Acir *et al.* [22] developed a novel SAC having circular turbulator collectors and investigated the energetic and exergetic performance. They used four black painted copper tubes having different obstacle relief angles ( $45^\circ$ ,  $90^\circ$ , and  $135^\circ$ ) inserted in the tube. Experiments were conducted at various  $\dot{m}$  which are 0.0023, 0.0033, 0.0044, and 0.0055 kg/s. They observed that the  $\eta_I$  ranges from 28.6% to 79.5% and  $\eta_{II}$  from 8.1% to 42.4%. The highest  $\eta_I$  and  $\eta_{II}$  were obtained at 0.0055 kg/s having  $45^\circ$  obstacle relief angle.

Neural model has been implemented by Ghritlahre and Prasad to estimate the  $\eta_I$  and  $\eta_{II}$  of SAH having roughened surface [23]. For this aim, first phase authors conducted experiments with mass flow rate from 0.010 to 0.0175 kg/s using roughened collector surface, and calculated the  $\eta_I$  and  $\eta_{II}$ . They used 60 sets of experimental data in neural model. In second phase, they developed a neural structure using 6 input variables, and 2 output variables as  $\eta_I$  and  $\eta_{II}$ , and four to seven neurons were selected at hidden layer. They trained the neural model using Levenberg–Marquardt training algorithm and found that the 6-6-2 neural model was optimal model for prediction. Abuşka developed a novel collector with conical sur-

face for SAH and conducted experiments with mass flow rate from 0.04 to 0.10 kg/s [24]. Using the thermodynamics concept of 1st and 2nd law, it was reported that the average  $\eta_I$  was obtained as 63.2% and 57.2% at 0.04 kg/s, 71.5% and 61.7% at 0.08 kg/s, and 74.6% and 64.0% at 0.10 kg/s on conical and smooth collector, respectively. Similarly, on the other side, the average  $\eta_{II}$  was obtained as 19.3% and 16.1% at 0.04 kg/s, 15.1% and 11.5% at 0.08 kg/s, and 12.5% and 9.2% at 0.1 kg/s on conical and smooth absorber surface, respectively. Also found that 10% enhancement in thermal performance as compared to conventional SAH.

Matheswaran *et al.* [25] analytically investigated  $\eta_I$  and  $\eta_{II}$  of SAC having single pass double duct jet surface. They coded a program in Matlab software for calculation of the energy and exergy efficiency. They developed a correlations for predicting  $\eta_{II}$  using the factors such as Reynolds number and design variables of jet plate. Aktaş *et al.* [26, 27] developed a novel design of SAH using multi-pass collector with perforated fins (MPSAC). They conducted experiments in two different conditions and examined the thermal and exergetic performances. The experiments were performed with  $\dot{m}$  using 0.0069 kg/s and 0.0087 kg/s. They reported that the  $\eta_I$  for double pass SAC varied from 30.37% to 69.03%, for MPSAC varied from 48.88% to 83.47%. Also reported  $\eta_{II}$  of double pass SAC and MPSAC were 2.10% and 17.12%, and 8.74% and 23.97%, respectively. Kumar and Layak analytically examined the thermal and exergy efficiency of SAH using twisted rib roughness on absorber plate [28]. They coded a program in Matlab software for calculation of the  $\eta_{th}$ , and  $\eta_{II}$ . They found that the maximum enhancement in  $\eta_{th}$ ,  $\eta_{II}$ , and  $\eta_{eff}$  and as 1.81, 1.81, and 1.79 times, respectively in comparison to the conventional SAH. Ural designed a novel type of flat plate SAH with textile fabric (TB) absorber surface [29]. This SAH performance was evaluated on the basis of energy and exergy analysis. To complete this aim, author conducted experiments with mass flow rate 0.028 kg/s and found that the energy and exergy efficiency of flat plate (FP) SAH as 53% and 31%, respectively. Similarly for TB-SAH as 70% and 41%, respectively. Also concluded that the exergy destruction rate of FP-SAH was higher than that of TB-SAH. Abdelkader *et al.* [30] experimentally studied the performance of novel type of flat-plate SAH coated with carbon nanotubes (CNTs) and cupric oxide nanoparticles embedded in a black paint. They reported that 4% CNTs/CuO-black paint is the highest solar selective coating with solar absorbance and thermal emittance reaches 0.964 and 0.124, respectively. They also found that the energy efficiency enhanced by approximately 24.4%. The difference between outlet and inlet

temperatures of the air across SAH rises up to 22% based on averaged values. Deep and Sreekumar fabricated a single pass parallel flow SAH with dimensions 2150 mm × 1100 mm × 150 mm to examine the energy and exergy performances [31]. They conducted experiments with five different air flow rates as 30, 45, 60, 75, and 90 kg/h m<sup>2</sup>. They found that the first and second laws of thermodynamic efficiency increase from 44.13% to 56.98% and from 24.98% to 36.62%, respectively, by increasing the flow rate from 30 to 90 kg/h m<sup>2</sup>. Also reported that the air flow duration inside the duct plays an important role in efficiency of the solar air heater. Therefore, at lower flow rate 30 kg/h m<sup>2</sup> the maximum outlet air temperature and temperature difference obtained as 80.7°C and 43.2°C, respectively. Debnath *et al.* [32] studied the energy and exergy analysis of plain and corrugated SAH. For this objective: they conducted experiments in two seasons mild winter (December) and hot summer (May–June) using single and double glazing collector. They performed experiments with  $\dot{m} = 3.9 - 11.8 \times 10^{-3}$  kg/s at tilt angles 30° and 45°. They reported that the double glazed collector enhances thermal efficiency by 2–4%. Authors also observed that the highest and lowest values of exergetic efficiency were found to be 0.44% and 17.3%, respectively. In addition to this, an enhanced thermal performance with tilt angle of 45°, and was more prominent during summer than that of winter. Ghritlahre *et al.* [33] developed artificial neural networks (ANN) model to predict the thermal performance of arc shaped roughened SAH using relevant input parameters. They also compared the ANN model performance with group method of data handling (GMDH) model and reported that the accurate prediction of ANN model is better than GMDH model. Ghritlahre studied the heat transfer and friction of roughened SAH using arc shaped wire rib roughness [34]. They reported that the heat transfer of apex upstream flow, averagely enhanced by 1.42 times, performs better than that of apex downstream flow. Ghritlahre and Vrema studied the prediction of exergetic performance of arc shaped wire rib roughened SAH using ANN model using relevant input parameters [35].

From the literature, it has been observed that the concept of 1st law (energy analysis) and 2nd law of thermodynamics (exergy analysis) have been used on various types of solar air heaters. Also observed that the experimental and analytical investigations of only apex downstream flow SAC having arc shaped wire roughness performances have been done by various researchers. But energy and exergy analysis of apex upstream and downstream flow roughened SAH duct performances are not yet done by any researchers. Due to this reason, in the present work 1st and 2nd laws of

thermodynamics have been considered for performance analysis of SAHs.

In the present study, for investigation of performance of SAH with downstream flow and upstream flow SAH duct have been designed and evaluated by experiments conducted at Jamshedpur city, in India. The main purpose of the current investigation is given as follows:

- (i) to conduct experiments with various mass flow rate using arc shaped roughened SAH,
- (ii) to evaluate the energy efficiency and exergy efficiency,
- (iii) to compare the performance of downstream and upstream flow.

## 2 Experimental setup

The apex downstream and upstream flow arc shaped roughened SAH was developed and fabricated at National Institute of Technology (NIT) Jamshedpur, and conducted experiments at actual outdoor condition of Jamshedpur City, in India. The detailed description of experimental setup is reported in Fig. 1.

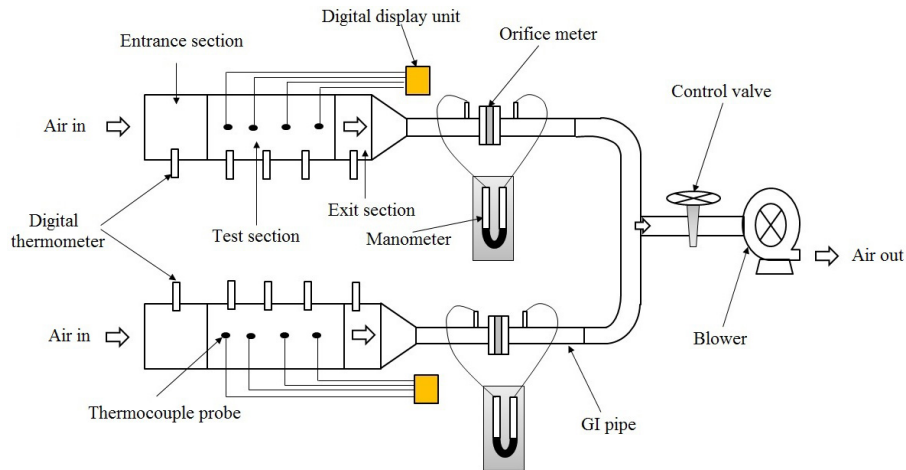


Figure 1: Schematic view of solar air heater setup.

It is clearly seen that the setup is structured with two ducts. In first duct the roughened absorber and in second duct smooth absorber plates have been used. The ducts have been fabricated with 2300 mm length, 330 mm

width and 35 mm height. The duct is separated in 3 sections: (i) entrance section, (ii) test section, and (iii) exit section. The absorber plate has been used in the test section. The galvanized iron (GI) sheet with 1 mm thickness was used for making the absorber plate. The photographs of experimental setup and absorber plate are given in Figs. 2 and 3, respectively. The various components which are used in the setup are suction blower, valve, orifice plate, U-tube manometer, glass cover, absorber plate, galvanized iron GI pipe, thermometers. The 63.5 mm GI pipe is connected with exit section of duct. The absorber plate specifications of roughness parameters are given in Table 1.

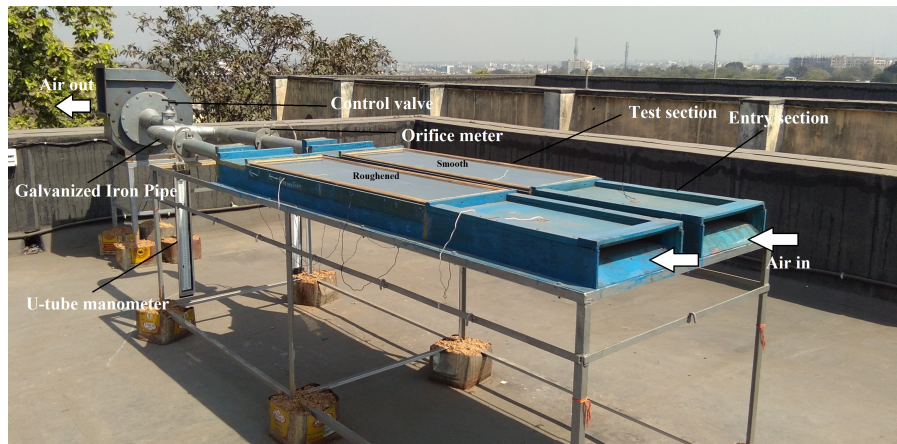


Figure 2: Experimental setup.

Table 1: Operating and roughness parameters.

Parameters	Value
Roughness size ( $e$ )	2.5 mm
Arc angle ( $\alpha$ )	60°
Relative roughness pitch ( $p/e$ )	10
Relative roughness height ( $e/D$ )	0.0395
Mass flow rate ( $\dot{m}_f$ )	0.007–0.022 kg/s

The 3-phase 5 high-pressure suction blower has been used to suck the air in the duct. Digital pyranometer has been used to measure the solar intensity and its photograph is shown in Fig. 4. The air temperature and absorber plate surface temperatures were measured by digital thermometers. The ex-

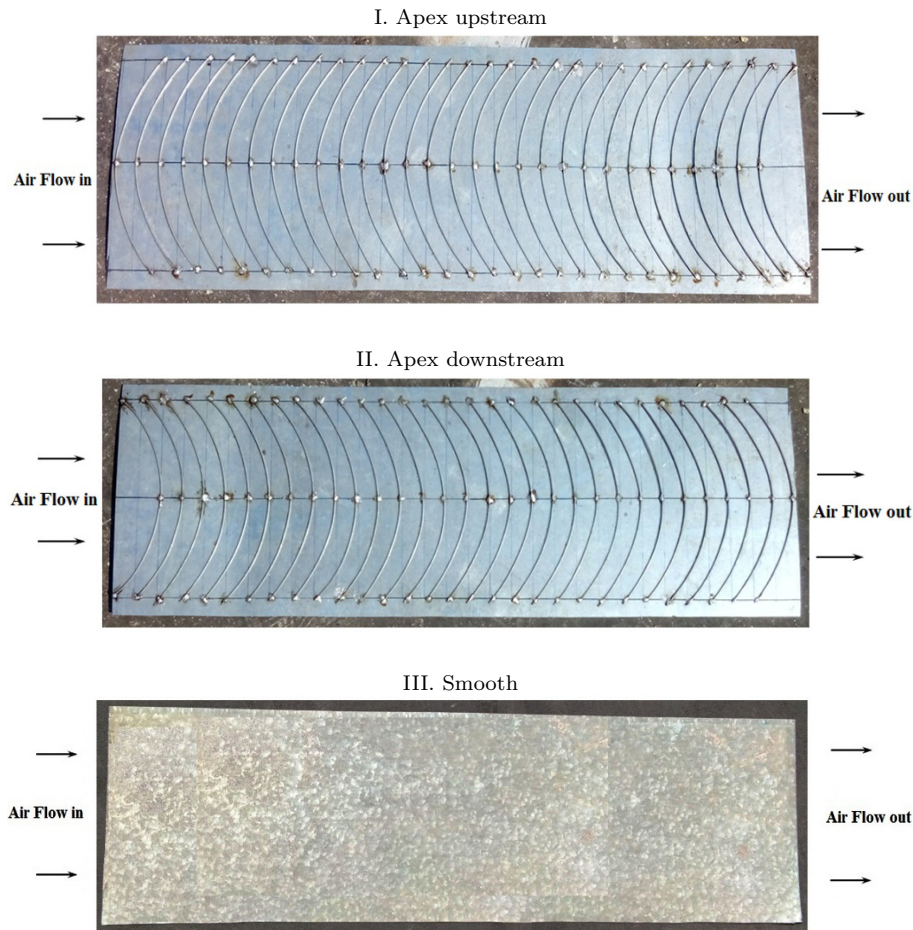


Figure 3: Photographs of absorber plates: I – apex upstream; II – apex downstream; III – smooth

periments were carried out using mass flow rate from 0.007 to 0.022 kg/s in the month of February–March 2017 and data has been collected from 9:00 to 16:00 hrs for analysis.

At the time of experiments, errors and uncertainties always arise during observation, reading, calibration and recording of the data, after applying the precaution during the measurements of data. These errors effects the results of experimental study. At the time of experiments various instruments were used to measure wind velocity, pressure drop, temperatures, solar intensity, diameter of pipe, length and width. Uncertainty analysis is needed



Figure 4: Digital pyranometer.

to prove the accuracy of the experiments. In this study, errors came from the sensitiveness of equipment and measurements uncertainties. Kline and McClintock developed the uncertainty analysis concept [36] which is used in present uncertainty analysis. In present study the uncertainty occurred in various instruments are reported in Table 2.

Considering the relative uncertainties in the individual factors by  $u_n$ ,

Table 2: Uncertainties in measurements.

Description	Error
Ambient air temperature	$\pm 0.16^\circ\text{C}$
Absorber plate temperature	$\pm 0.16^\circ\text{C}$
Collector outlet temperature	$\pm 0.16^\circ\text{C}$
Collector inlet temperature	$\pm 0.16^\circ\text{C}$
Pressure drop across the orifice plate	$\pm 1$ mm
Air velocity	$\pm 0.14$ m/s
Solar energy	$\pm 0.1$ W/m <sup>2</sup>
Vernier calliper	0.2 m
Linear scale	$\pm 1$ mm
Reading the values of table	$\pm 0.1-0.2\%$

the total uncertainty could be calculated by the relation [37]:

$$U = [(u_1)^2 + (u_2)^2 \dots (u_n)^2]^{1/2}. \quad (1)$$

Uncertainties of useful heat gain and mass flow rate were obtained as  $\pm 3.36\%$  and  $\pm 0.876\%$ , respectively.

### 3 Thermal and exergy analysis of solar air heater

#### 3.1 Thermal analysis

The thermal performance of solar air heater is evaluated on the first law of thermodynamics [1,2]. This is represented in terms of thermal efficiency which is the ratio between useful heat gain by air and solar radiation incident on collector surface. The thermal efficiency of solar air heater is expressed by

$$\eta_{th} = \frac{\dot{Q}_u}{\dot{Q}_c}, \quad (2)$$

where the useful heat gain is denoted by  $\dot{Q}_u$  and the incident solar radiation by  $\dot{Q}_c$ . These terms are calculated by following formulas:

$$\dot{Q}_u = \dot{m}_f C_p \Delta T_f = \dot{m}_f C_p (T_{fo} - T_{fi}), \quad (3)$$

$$\dot{Q}_c = I A_p, \quad (4)$$

where  $\dot{m}_f$  is mass flow rate,  $C_p$  is specific heat (air),  $T_f$  is the temperature of fluid (air),  $I$  is the solar irradiance and  $A_p$  is collector surface area.

According to Eq. (2) the thermal efficiency is calculated by using the given equations [1,2,40]:

$$\eta_{th} = \frac{\dot{m}_f C_p (T_{fo} - T_{fi})}{I A_p}. \quad (5)$$

#### 3.2 Exergy analysis

The exergy analysis is evaluated on the basis of the second law of thermodynamics. The concept of exergy is very useful for optimal use of energy and this can be used for designing of thermal systems for efficient utilization in their operations. The ratio between the exergy gained and exergy input is called as exergetic efficiency and it is denoted by  $\eta_{II}$ .

During the exergy analysis, the following assumptions are applied [35, 39]:

- The system is considered to be in steady state condition.
- Neglecting the chemical and nuclear reactions.
- Neglecting the kinetic energy and potential energy.
- Consider the specific heat of air is constant and it works as an ideal fluid.

In general, energy and exergy balance equations are [7–9]:

$$\sum \dot{E}_i = \sum \dot{E}_o, \quad (6)$$

$$\sum \dot{E}x_i - \sum \dot{E}x_o = \sum \dot{E}x_{loss}, \quad (7)$$

where

$$\begin{aligned} \sum \dot{E}x_{loss} &= \sum \dot{E}x_{loss(ext)} + \sum \dot{E}x_{loss(int)} = \sum \dot{E}x_{loss(ext)} \\ &+ \sum \dot{E}x_{dest}, \end{aligned} \quad (8)$$

$$\begin{aligned} \sum \dot{E}x_{dest} &= \sum \dot{E}x_{heat} - \sum \dot{E}x_{work} + \sum \dot{E}x_{mass,in} \\ &- \sum \dot{E}x_{mass,out} - \sum \dot{E}x_{loss(ext)}. \end{aligned} \quad (9)$$

The Eq. (9) can also be represented by

$$\sum \dot{E}x_{dest} = \sum \dot{E}x_{heat} - W + \sum m_i \psi_i - \sum m_o \psi_o - \sum \dot{E}x_{loss(ext)}. \quad (10)$$

In Eqs. (6)–(10),  $\dot{E}$  is energy rate and  $\dot{E}x$  is exergy rate. Using the Petela theorem  $\sum \dot{E}x_{heat}$  can be given as [38]

$$\sum \dot{E}x_i = \sum \dot{E}x_{heat} = IA_p \left[ 1 - \frac{4}{3} \left( \frac{T_a}{T_s} \right) + \frac{1}{3} \left( \frac{T_a}{T_s} \right)^4 \right], \quad (11)$$

where  $T_a$  and  $T_s$  stand for atmospheric temperature and sun surface temperature, respectively. Now the specific exergy at inlet and outlet can be represented by the following equations:

$$\psi_i = (h_i - h_e) - T_e(s_i - s_e), \quad (12)$$

$$\psi_o = (h_o - h_e) - T_e(s_o - s_e). \quad (13)$$

In Eqs. (12) and (13), enthalpy is denoted by  $h$  and entropy by  $s$ , suffix  $e$  stands for the environment.

The external loss term in Eq. (10) is calculated by using following relation [7]:

$$\begin{aligned} \sum \dot{E}x_{loss(ext)} &= \sum \dot{E}x_{loss(opt)} \\ &= (1 - \tau\alpha)IA_p \left[ 1 - \frac{4}{3} \left( \frac{T_a}{T_s} \right) + \frac{1}{3} \left( \frac{T_a}{T_s} \right)^4 \right]. \end{aligned} \quad (14)$$

From Eqs. (11) to (14) using in Eq. (10), then the resulting equation becomes:

$$\begin{aligned} \left[ 1 - \frac{4}{3} \left( \frac{T_a}{T_s} \right) + \frac{1}{3} \left( \frac{T_a}{T_s} \right)^4 \right] Q_c - m_f [(h_o - h_i) - T_a(s_o - s_i)] \\ - (1 - \tau\alpha)IA_p \left[ 1 - \frac{4}{3} \left( \frac{T_a}{T_s} \right) + \frac{1}{3} \left( \frac{T_a}{T_s} \right)^4 \right] = \sum \dot{E}x_{dest}, \end{aligned} \quad (15)$$

where  $\dot{Q}_c$  is calculated by Eq. (4) and  $W = 0$ .

The changes in enthalpy and entropy of air can be given respectively as:

$$\Delta h_{air} = h_o - h_i = C_p (T_{fo} - T_{fi}), \quad (16)$$

$$\Delta s_{air} = s_o - s_i = C_p \ln \frac{T_{fo}}{T_{fi}} - R \ln \frac{P_o}{P_i}, \quad (17)$$

where  $R$  is a universal gas constant and  $P$  is pressure.

Putting Eqs. (4), (16) to (18) in Eq. (15), the following expression is obtained:

$$\begin{aligned} \left[ 1 - \frac{4}{3} \left( \frac{T_a}{T_s} \right) + \frac{1}{3} \left( \frac{T_a}{T_s} \right)^4 \right] IA_p - m_f C_p (T_{fo} - T_{fi}) \\ + m_f T_a \left( C_p \ln \frac{T_{fo}}{T_{fi}} - R \ln \frac{P_o}{P_i} \right) \\ - (1 - \tau\alpha)IA_p \left[ 1 - \frac{4}{3} \left( \frac{T_a}{T_s} \right) + \frac{1}{3} \left( \frac{T_a}{T_s} \right)^4 \right] = \sum \dot{E}x_{dest}. \end{aligned} \quad (18)$$

The exergetic efficiency of SAH can be formulated by the ratio of net exergy output of the system to exergy input of the system [7]

$$\eta_{II} = \frac{\sum \dot{E}x_o}{\sum \dot{E}x_i} = 1 - \frac{\sum \dot{E}x_{loss}}{\sum \dot{E}x_i}. \quad (19)$$

## 4 Results and discussions

In this study, the apex downstream and upstream flow roughened solar air heater having arc shaped wire rib have been designed to improve the SAH performance. To evaluate the performance of SAHs, experiments were carried out at NIT Jamshedpur from 22 Feb. 2017 to 05 March 2017 in clear sky of Jamshedpur city, which is located at  $22.77^{\circ}\text{N}$  and  $86.14^{\circ}\text{E}$ , India. Experiments were performed with mass flow rate from  $0.007\text{ kg/s}$  to  $0.022\text{ kg/s}$ . The wind speed varies from  $0.3\text{ m/s}$  to  $4.8\text{ m/s}$  in all experimental days. There are three different absorber plates which have been used in the experiments. First absorber plate is apex upstream flow, second is downstream flow and the last absorber plate is smooth surface which are shown in Fig. 3.

The variation of atmospheric temperature, wind speed and solar intensity are shown in Fig. 5. It has been observed that the solar intensity is maximum between 12:00 hr to 13:00 hr, firstly solar intensity increases up at 12:00 hr and then starts decreasing. At local weather condition, the variation of ambient temperature, outlet air temperature and wind speed of 6 days (28th Feb.–05th Mar. 2017) is given in Fig. 6. The maximum wind speed of  $4.8\text{ m/s}$  observed on date 01 March 2017 and avg. wind speed was

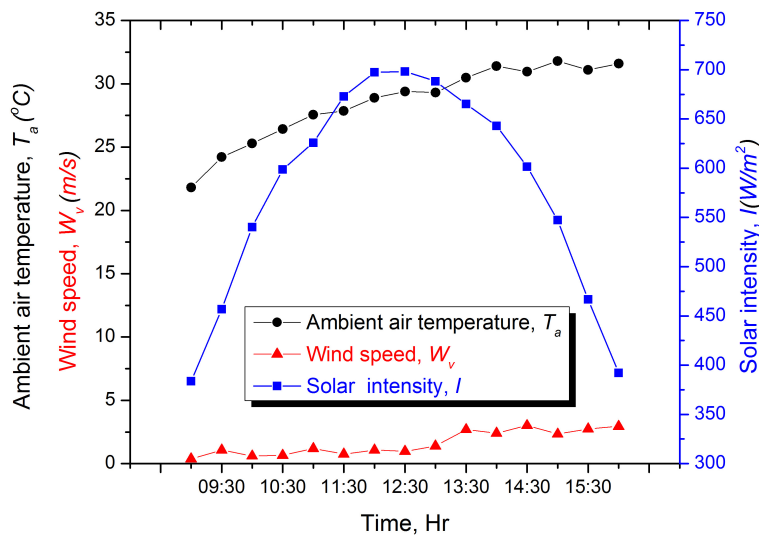


Figure 5: The variation of ambient temperature, wind speed and solar intensity on 22 Feb. 2017.

2.6 m/s. In case of ambient temperature, maximum temperature  $35.8^{\circ}\text{C}$  observed on 28th Feb. 2017 and avg.  $32.5^{\circ}\text{C}$ .

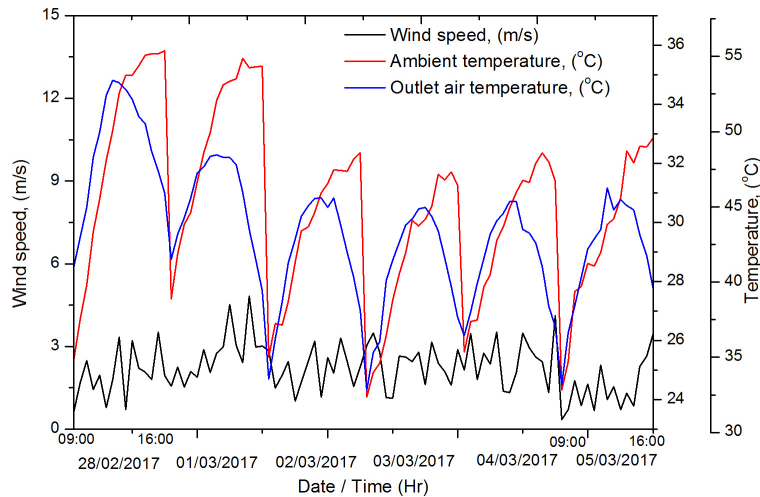
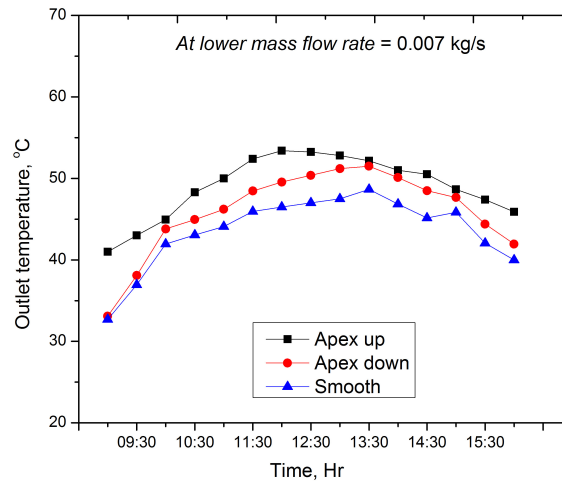


Figure 6: Wind speed, ambient temperature and outlet air temperature (28th Feb.–05th March 2017).

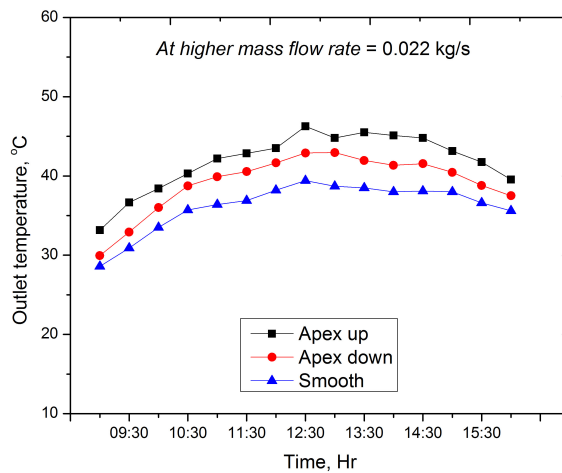
#### 4.1 Effect of mass flow rate on outlet air temperature

The effect of mass flow rate on the outlet air temperature is shown in Fig. 7. From this figure, it is clear that the outlet air temperature of smooth absorber plate based solar air heater is very low as compared to apex downstream and apex upstream flow solar air heater. The maximum outlet temperature has been found for apex upstream flow as  $53.4^{\circ}\text{C}$ . Similarly for downstream flow and smooth duct SAH obtained as  $51.5^{\circ}\text{C}$  and  $47.8^{\circ}\text{C}$ , respectively. These results were found at minimum mass flow rate. In case of higher mass flow rate, for apex upstream flow the maximum temperature was obtained as  $46.2^{\circ}\text{C}$ . Similarly for downstream flow and smooth duct SAH obtained were  $42.9^{\circ}\text{C}$  and  $38.9^{\circ}\text{C}$ , respectively.

From the above results, it is found that the mass flow rate of air greatly affects the outlet air temperature. If mass flow rate is increased then the outlet air temperatures will be goes down and becomes equal to the ambient air temperature. Thus, the mass flow rate should decreases for obtaining increased values of outlet air temperature. In current study, the maximum outlet temperature obtained at lower mass flow rate ( $0.007\text{ kg/s}$ ).



(a)



(b)

Figure 7: Effects on outlet air temperatures at (a) minimum 0.007 kg/s and (b) maximum 0.022 kg/s mass flow rate.

## 4.2 Thermal and exergy analysis of upstream and downstream flow solar air heater

Performances of SAHs have been evaluated on the basis of 1st and 2nd laws of thermodynamics. For this analysis, during the experiments ambient temperature, outlet air temperature, inlet air temperature, absorber plate temperature and solar intensity data have been recorded. These data were

collected from 22th Feb. to 5th March 2017. Data were recorded daily 15 times at 30 min interval from morning 9:00 hr to evening 16:00 hr. Using these data, the thermal efficiency and exergy efficiency is calculated by using Eqs. (5) and (18), respectively. These efficiencies were calculated with the mass flow rate ranging from 0.007 kg/s to 0.022 kg/s. Figure 8 shows

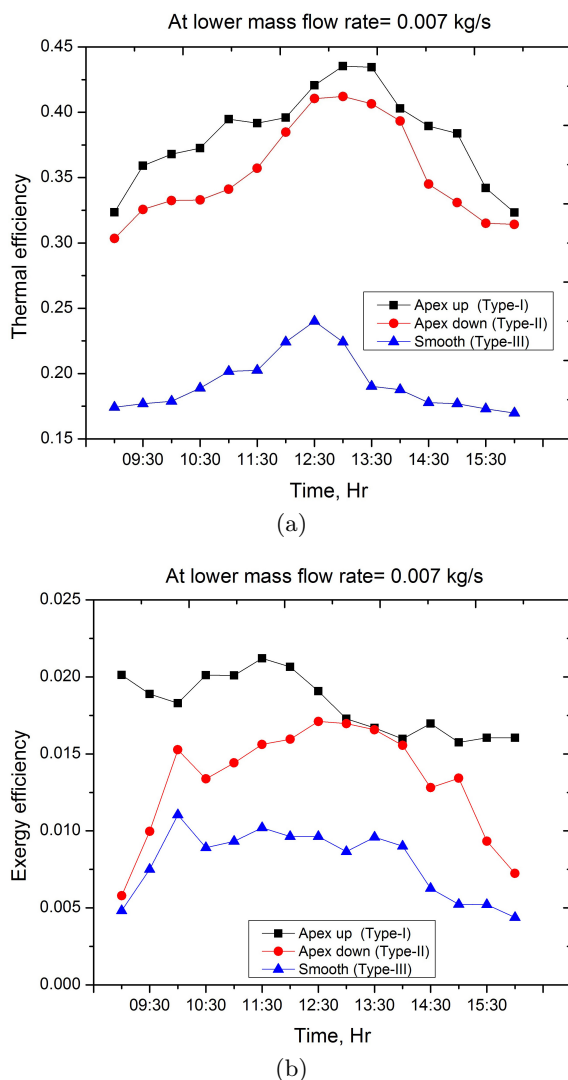
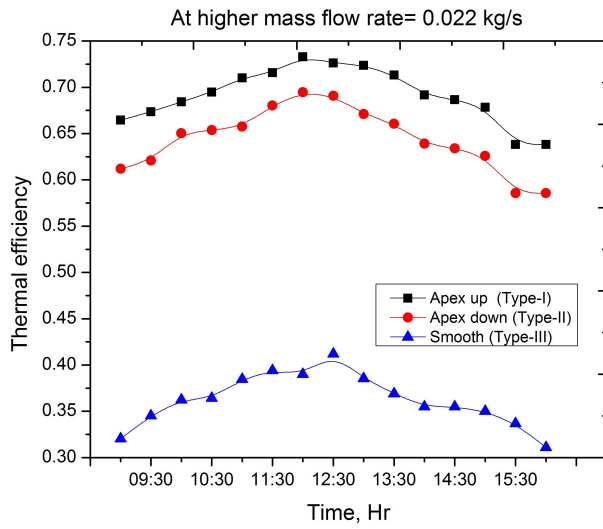
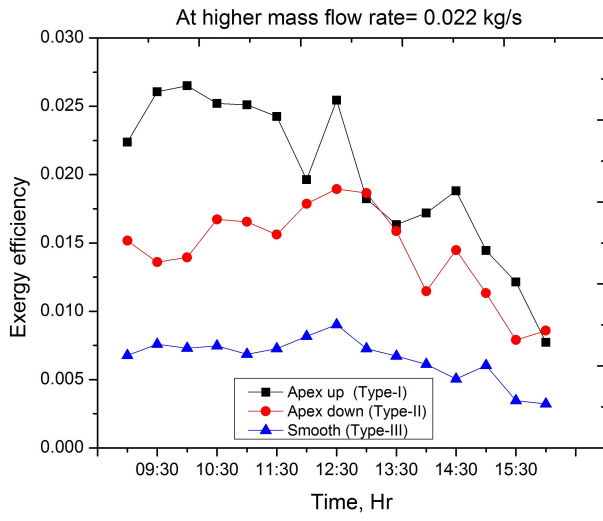


Figure 8: Variations of efficiency at lower mass flow rate 0.007 kg/s: (a) energy efficiency; (b) exergy efficiency.

the hourly variation of thermal and exergy efficiencies of all three different types of SAHs at lower mass flow rate 0.007 kg/s. Similarly Fig. 9 shows the variations at higher mass flow rate 0.022 kg/s. From Fig. 8, it has been



(a)



(b)

Figure 9: Variation of efficiency at higher mass flow rate 0.022 kg/s: (a) thermal efficiency; (b) exergy efficiency.

obtained that the average thermal efficiency of apex upstream, downstream and smooth duct SAH are found to be 38.2%, 35.3%, and 20.2%, respectively, and similarly in case of exergy efficiency the average value were 1.8%, 1.3%, and 0%, respectively. At maximum mass flow rate, the average thermal efficiency were found as 69.1%, 64.4%, and 38.1%, respectively. The average exergy efficiency have been obtained as 1.9%, 1.4%, and 0.6% for type-I, type-II, and type-III, respectively.

The thermal and exergy efficiencies of each type of solar air heater have been given in Table 3. From the table, it is found that the maximum thermal efficiency and exergy efficiency is 73.2% and 2.64%, respectively at higher mass flow rate (0.022 kg/s) for apex upstream flow SAH. In case of downstream flow the maximum thermal efficiency and exergy efficiency observed as 69.4% and 1.89%, respectively for same mass flow rate. Also found that the maximum values of  $\eta_{th}$  and  $\eta_{II}$  as 43.4% and 0.9%, respectively for smooth duct SAH.

Table 3: Energy and exergy analysis of upstream, downstream flow and smooth duct SAHs.

Mass flow rate ( $\dot{m}$ , kg/s)	Type	Thermal efficiency, %		Exergy efficiency, %	
		Min.	Max.	Min.	Max.
0.007	Type-I (Apex up)	32.4	43.5	1.57	2.12
	Type-I (Apex down)	30.5	41.0	0.57	1.71
	Type-III (Smooth)	17.3	25.2	0.43	1.10
0.022	Type-I (Apex up)	63.3	73.2	0.77	2.64
	Type-I (Apex down)	56.5	69.4	0.78	1.89
	Type-III (Smooth)	31.2	43.3	0.32	0.91

The comparative graph of solar air heater with upstream and downstream flow is given in Fig. 10. As seen from the figure, it is concluded that the solar air heater with apex upstream flow performs better than apex downstream flow. This is because more turbulence occurs in apex upstream flow as compared to downstream flow. The dispersion of air flow is more in the upstream flow.

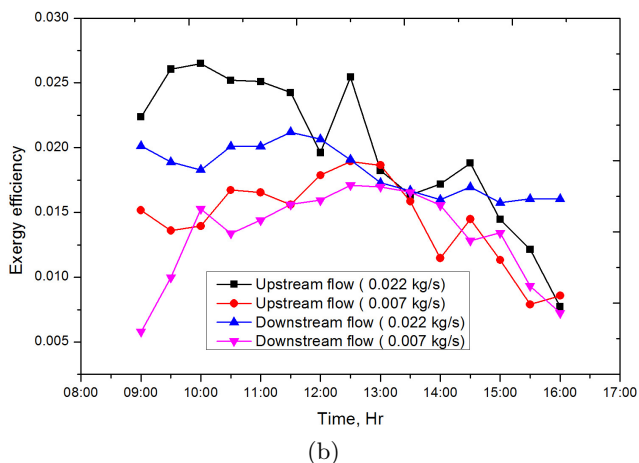
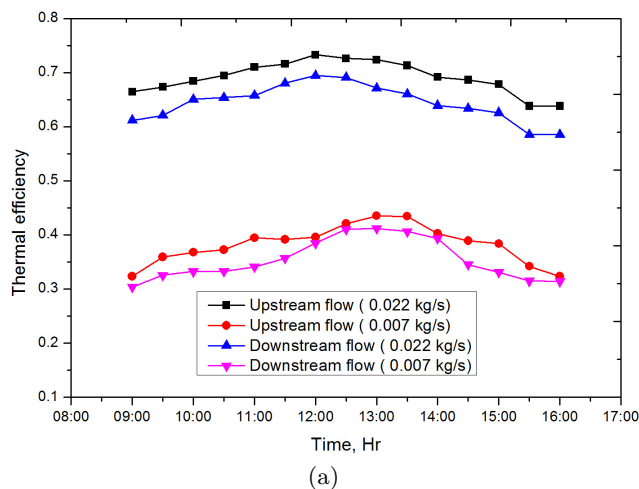


Figure 10: Comparative variation of apex upstream flow and downstream flow duct solar air heaters.

## 5 Conclusions

In the present work, experimental study has been conducted to evaluate energy and exergy efficiencies of three different types of solar air heaters under various operating conditions. These three types are: (i) apex downstream flow SAH, (ii) upstream flow SAH, and (iii) flat surface SAH. For examination of energetic and exergetic performances, experiments were performed with various mass flow rates of air ranging from 0.007 to 0.022 kg/s.

According to the results the following conclusions have been drawn:

- It has been found that the efficiency of the solar air heaters significantly depends on the solar radiation and absorber plate surface geometry.
- The thermal and exergy efficiency leads with increases in mass flow rate from 0.007 to 0.022 kg/s.
- At apex upstream flow SAH the maximum outlet temperature of air is found to be as 53.4°C at minimum mass flow rate of 0.007 kg/s.
- The maximum thermal efficiency  $\eta_{th}$  and exergy efficiency  $\eta_{II}$  obtained as 73.2% and 2.64%, respectively for apex upstream flow at 0.022 kg/s.
- In case of downstream flow: the maximum thermal efficiency and exergy efficiency were obtained as 69.4% and 1.89%, respectively.

In view of the above results, it is clearly understood that the apex upstream flow SAH performs better than apex downstream flow SAH. In the upstream flow with arc shaped wire rib roughened SAH, the thermal efficiency values are found to be higher because there is more dispersion of flow in this case as compared to apex downstream flow, which causes more turbulence in the flow.

**Acknowledgements** The Author expresses great thankfulness to Mechanical Engineering Department of NIT Jamshedpur for allowing to conduct experiments and for providing necessary laboratory facility.

*Received 17 April 2021*

## References

- [1] DUFFIE J.A., BECKMAN W.A.: *Solar Engineering of Thermal Processes* (3rd Edn.). Wiley, New York 2006.
- [2] GARG H.P., PRAKASH J.: *Solar Energy Fundamentals and Applications*. Tata McGraw Hill, New Delhi 2006.
- [3] GHRITLAHRE H.K.: *Performance Evaluation of solar air heating systems using artificial neural network*. PhD thesis, National Institute of Technology, Jamshedpur 2019.

- [4] GHRITLAHRE H.K., CHANDRAKAR P., AHMAD A.: *A comprehensive review on performance prediction of solar air heaters using artificial neural network*. Ann. Data Sci. **8**(2019), 405–449.
- [5] PRAKASH C., SAINI R.P.: *Use of artificial roughness for performance enhancement of solar air heaters – a review*. Int. J. Green Energy **16**(2019), 7, 551–572.
- [6] GHRITLAHRE H.K., SAHU P.K., CHAND S.: *Thermal performance and heat transfer analysis of arc shaped roughened solar air heater – An experimental study*. Sol. Energy **199**(2020), 173–182.
- [7] GHRITLAHRE HK, PRASAD RK.: *Exergetic performance prediction of a roughened solar air heater using artificial neural network*. Strojniški vestnik/J. Mech. Eng. **64**(2018), 3, 195–206.
- [8] GHRITLAHRE H.K., PRASAD R.K.: *Exergetic performance prediction of solar air heater using MLP, GRNN and RBF models of artificial neural network technique*. J. Environ. Manage. **223**(2018), 566–575.
- [9] GHRITLAHRE H.K., PRASAD R.K.: *Prediction of exergetic efficiency of artificial arc shape roughened solar air heater using ANN model*. Int. J. Heat Technol. **36**(2018), 3, 1107–1115.
- [10] KURTBAS I., DURMUS A.: *Efficiency and exergy analysis of a new solar air heater*. Renew. Energ. **29**(2004), 9, 1489–1501.
- [11] KURTBAS I, TURGUT E.: *Experimental investigation of solar air heater with free and fixed fins: Efficiency and exergy loss*. Int. J. Sci. Technol. **1**(2006), 1, 75–82.
- [12] KARSLI S.: *Performance analysis of new-design solar air collectors for drying applications*. Renew. Energ. **32**(2007), 10, 1645–1660.
- [13] ESEN H.: *Experimental energy and exergy analysis of a double-flow solar air heater having different obstacles on absorber plates*. Build. Environ. **43**(2008), 6, 1046–1054.
- [14] GUPTA M.K., KAUSHIK S.C.: *Exergetic performance evaluation and parametric studies of solar air heater*. Energy **33**(2008), 11, 1691–1702.
- [15] GUPTA M.K., KAUSHIK S.C.: *Performance evaluation of solar air heater for various artificial roughness geometries based on energy, effective and exergy efficiencies*. Renew. Energ. **34**(2009), 3, 465–476.
- [16] AKPINAR E.K., KOÇYIĞIT F.: *Energy and exergy analysis of a new flat-plate solar air heater having different obstacles on absorber plates*. Appl. Energ. **87**(2010), 11, 3438–3450.
- [17] ALTA D., BILGILI E., ERTEKIN C., YALDIZ O.: *Experimental investigation of three different solar air heaters: energy and exergy analyses*. Appl. Energ. **87**(2010), 10, 2953–2973.
- [18] BOUADILA S., KOOLI S., LAZAAR M., SKOURI S., FARHAT A.: *Performance of a new solar air heater with packed-bed latent storage energy for nocturnal use*. Appl. Energ. **110**(2013), 267–275.
- [19] BENLI H.: *Experimentally derived efficiency and exergy analysis of a new solar air heater having different surface shapes*. Renew. Energ. **50**(2013), 58–67.

- [20] BAYRAK F., OZTOP H.F., HEPBASLI A.: *Energy and exergy analyses of porous baffles inserted solar air heaters for building applications*. *Energ. Buildings* **57**(2013), 338–345.
- [21] VELMURUGANA P., KALAIVANAN R.: *Energy and exergy analysis of multi-pass flat plate solar air heater – An analytical approach*. *Int. J. Green Energy* **12**(2015), 8, 810–820.
- [22] ACIR A., ATA I., ŞAHİN I.: *Energy and exergy analyses of a new solar air heater with circular-type turbulators having different relief angles*. *Int. J. Exergy* **20**(2016), 1, 85–104.
- [23] GHRTLAHRE H.K., PRASAD R.K.: *Energetic and exergetic performance prediction of roughened solar air heater using artificial neural network*. *Cienc. Tec. Vitivinic.* **32**(2017), 11, 2–24
- [24] ABUŞKA M.: *Energy and exergy analysis of solar air heater having new design absorber plate with conical surface*. *Appl. Therm. Eng.* **131**(2018), 115–124.
- [25] MATHESWARAN M.M., ARJUNAN T.V., SOMASUNDARAM D.: *Analytical investigation of solar air heater with jet impingement using energy and exergy analysis*. *Sol. Energy* **161**(2018), 25–37.
- [26] AKTAŞ M. ŞEVIK S., DOLGUN E.C., DEMIRCI B.: *Drying of grape pomace with a double pass solar collector*. *Dry. Technol.* **37**(2019), 1, 105–117.
- [27] AKTAŞ M., SÖZEN A., TUNCER A.D., ARSLAN E., KOŞAN M., ÇÜRÜK O.: *Energy-exergy analysis of a novel multi-pass solar air collector with perforated fins*. *Int. J. Renew. Energ. Dev.* **8**(2019), 1, 47–55.
- [28] KUMAR A., LAYEK A.: *Energetic and exergetic performance evaluation of solar air heater with twisted rib roughness on absorber plate*. *J. Clean. Prod.* **232**(2019), 617–628.
- [29] URAL T.: *Experimental performance assessment of a new flat-plate solar air collector having textile fabric as absorber using energy and exergy analyses*. *Energy* **188**(2019), 116116.
- [30] ABDELKADER T.K., ZHANG Y., GABALLAH E.S., WANG S., WAN Q., FAN Q.: *Energy and exergy analysis of a flat-plate solar air heater coated with carbon nanotubes and cupric oxide nanoparticles embedded in black paint*. *J. Clean. Prod.* **250**(2020), 19501.
- [31] DHEEP G.R., SREEKUMAR A.: *Experimental studies on energy and exergy analysis of a single pass parallel flow solar air heater*. *J. Sol. Energy Eng.* **142**(2020), 1, 011003 SOL-19-1038 .
- [32] DEBNATH S., DAS B., RANDIVE P.: *Energy and exergy analysis of plain and corrugated solar air collector: effect of seasonal variation*. *Int. J. Amb. Energ.* (2020), doi: [10.1080/01430750.2020.1778081](https://doi.org/10.1080/01430750.2020.1778081).
- [33] GHRTLAHRE H.K., CHANDRAKAR P., AHMAD A.: *Application of ANN model to predict the performance of solar air heater using relevant input parameters*. *Sustain. Energ. Technol. Asses.* **40**(2020), 100764.
- [34] GHRTLAHRE H.K.: *Heat transfer and friction factor characteristics investigation of roughened solar air heater using arc shaped wire rib roughness*. *Int. J. Amb. Energ.* (2021), doi: [10.1080/01430750.2021.1934115](https://doi.org/10.1080/01430750.2021.1934115).

- [35] GHRIHLAHRE H.K., VERMA M.: *Accurate prediction of exergetic efficiency of solar air heaters using various predicting methods*. J. Clean. Prod. **288**(2021), 125115.
- [36] KLINE S.J., MCCLINTOCK F.A.: *Describe uncertainties in single sample experiments*. Mech. Eng. **75**(1953), 1, 3–8.
- [37] HOLMAN J.P.: *Experimental Methods for Engineers*. McGraw-Hill, New York 2007.
- [38] PETELA R.: *An approach to the exergy analysis of photosynthesis*. Sol. Energy, **82**(2008), 4, 311–328.
- [39] GHRIHLAHRE H.K., SAHU P.K.: *A comprehensive review on energy and exergy analysis of solar air heaters*. Arch. Thermodyn. **41**(2020), 3, 183–222.
- [40] GHRIHLAHRE H.K., CHANDRAKAR P., AHMAD A.: *Solar air heater performance prediction using artificial neural network technique with relevant input variables*. Arch. Thermodyn. **41**(2020), 3, 255–282.